Document made available under the Patent Cooperation Treaty (PCT)

International application number: PCT/GB04/005216

International filing date: 14 December 2004 (14.12.2004)

Document type: Certified copy of priority document

Document details: Country/Office: GB
Number: 0329206.7
Filing date: 17 December 2003 (17.12.2003)

Date of receipt at the International Bureau: 24 January 2005 (24.01.2005)

Remark: Priority document submitted or transmitted to the International Bureau in compliance with Rule 17.1(a) or (b)

PCT/GB 2004 / 0 0 5 2 1 6

The Patent Office
Concept House
Cardiff Road
Newport
South Wales
NP10 8QQ

I, the undersigned, being an officer duly authorised in accordance with Section 74(1) and (4) of the Deregulation & Contracting Out Act 1994, to sign and issue certificates on behalf of the Comptroller-General, hereby certify that annexed hereto is a true copy of the documents as originally filed in connection with the patent application identified therein.

In accordance with the Patents (Companies Re-registration) Rules 1982, if a company named in this certificate and any accompanying documents has re-registered under the Companies Act 1980 with the same name as that with which it was registered immediately before re-registration save for the substitution as, or inclusion as, the last part of the name of the words "public limited company" or their equivalents in Welsh, references to the name of the company in this certificate and any accompanying documents shall be treated as references to the name with which it is so re-registered.

In accordance with the rules, the words "public limited company" may be replaced by p.l.c., plc, P.L.C. or PLC.

Re-registration under the Companies Act does not constitute a new legal entity but merely subjects the company to certain additional company law rules.

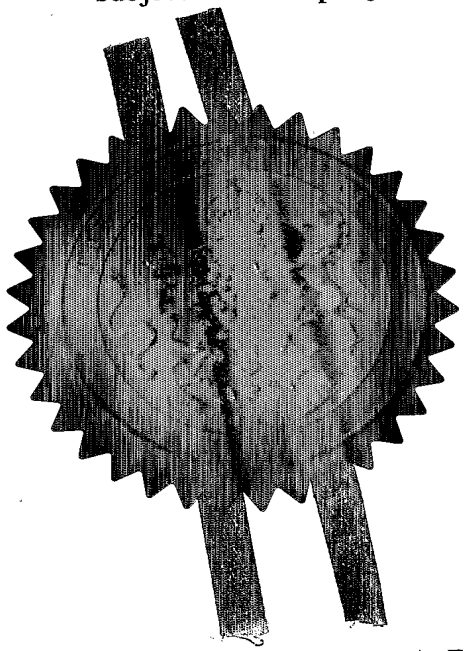

Signed

Dated 11 January 2005

nts Form 1/77

Patents Act 1977
(Rule 16)

The Patent Office

1/77

17DEC03 E860208-1 D02806
P01/7700 0.00-0329206.7 ACCOUNT CHA

THE PATENT OFFICE
C
17 DEC 2003
NEWPORT

The Patent Office

Cardiff Road
Newport
Gwent
NP10 8QQ

Request for grant of a patent

(See the notes on the back of this form. You can also get an explanatory leaflet, from the Patent Office to help you fill in this form)

1. Your reference — GML2915

2. Patent application number *(The Patent Office will fill in this part)* — 0329206.7 — 17 DEC 2003

3. Full name, address and postcode of the or of each applicant *(underline all surnames)*

UNIVERSITY OF SOUTHAMPTON
Highfield
Southampton
Hampshire
SO17 1BJ
GB

Patents ADP number *(if you know it)* 7984700001

If the applicant is a corporate body, give the country/state of its incorporation

4. Title of the invention — INERTIAL ACTUATOR

5. Name of your agent *(if you have one)*

"Address for service" in the United Kingdom to which all correspondence should be sent *(including the postcode)*

Barker Brettell
Medina Chambers
Town Quay
Southampton SO14 2AQ

Patents ADP number *(if you know it)* 07442494001 ✓

6. If you are declaring priority from one or more earlier patent applications, give the country and the date of filing of the or of each of these earlier applications and *(if you know it)* the or each application number

Country	Priority application number *(if you know it)*	Date of Filing *(day/month/year)*

7. If this application is divided or otherwise derived from an earlier UK application, give the number and the filing date of the earlier application

Number of earlier application	Date of filing *(day/month/year)*

8. Is a statement of inventorship and of right to grant of a patent required in support of this request *(Answer 'Yes' if:*
a) any applicant named in part 3 is not an inventor, or
b) there is an inventor who is not named as an applicant, or
c) any named applicant is a corporate body.
See note (d))

YES

Patents Form 1/77

9. Enter the number of sheets for any of the following items you are filing with this form. Do not count copies of the same document

Continuation sheets of this form	
Description	27
Claim(s)	3
Abstract	
Drawing(s)	10 + 10 RM

10. If you are also filing any of the following, state how many against each item.

Priority documents	
Translations of priority documents	
Statement of inventorship and right to grant of a patent *(Patents Form 7/77)*	
Request for preliminary examination *(Patents Form 9/77)*	
Request for substantive examination *(Patents Form 10/77)*	
Any other documents *(please specify)*	

11. I/We request the grant of a patent on the basis of this application.

Signature: Barker Brettell

Date: 16/12/03

12. Name and daytime telephone number of person to contact in the United Kingdom: G.M Lomas 023 8033 6970

Warning

After an application for a patent has been filed, the Comptroller of the Patent Office will consider whether publication or communication of the invention should be prohibited or restricted under Section 22 of the Patents Act 1977. You will be informed if it is necessary to prohibit or restrict your invention in this way. Furthermore, if you live in the United Kingdom, Section 23 of the Patents Act 1977 stops you from applying for a patent abroad without first getting written permission from the Patent Office unless an application has been filed at least 6 weeks beforehand in the United Kingdom for a patent for the same invention and either no direction prohibiting publication or communication has been given, or any such direction has been revoked.

Notes

a) If you need help to fill in this form or you have any questions, please contact the Patent Office on 01645 500505

b) Write your answers in capital letters using black ink or you may type them.

c) If there is not enough space for all the relevant details on any part of this form, please continue on a separate sheet of paper and write "see continuation sheet" in the relevant part(s). Any continuation sheet should be attached to this form.

d) If you have answered 'Yes' Patents Form 7/77 will need to be filed.

e) Once you have filled in the form you must remember to sign and date it.

f) For details of the fee and ways to pay please contact the Patent Office.

INERTIAL ACTUATOR

The present invention relates to inertial actuators, and in particular to their use in active vibration control systems.

INTRODUCTION

Vibration and noise occur in most machines, structures and dynamic systems. This leads to many undesirable consequences such as degraded performance, structural fatigue, decreased reliability, and human discomfort. There are two main classes of noise and vibration isolation systems which aim to reduce the level of noise and vibration induced by a mechanical structure: passive vibration control and active vibration control.

Passive vibration control involves the use of a resilient mount to isolate a structure from another structure which is vibrating. However, with such passive mounts there is a trade off between low and high frequency performance, with the mount reducing vibrations at low frequencies, but reducing isolation at high frequencies.

Active isolation systems such as Skyhook Damping may be used to achieve a more satisfactory compromise. These cause an actuator to generate a force to compensate for the vibrations and so reduce their transmission to the structure under control. This works well with reactive actuators, but because these need to react off a base structure they can be difficult to implement and are prone to displacement by horizontal forces. Inertial actuators are preferable since they can be directly installed on a vibrating structure. In practice, however, active damping using an inertial actuator is only semi-stable and vibration isolation at low frequencies is difficult to achieve due to the system's instability.

It has been shown that in order to implement stable skyhook damping with an inertial actuator, the natural frequency of the actuator must be below the first resonant frequency of the structure under control and the actuator resonance should be well damped [4]. In practice this is difficult to achieve as low resonant frequencies correspond to mounts which are dynamically 'soft'. These are prone to 'sag' under a static acceleration such as gravity, reducing the efficiency of the actuator.

The present invention seeks to substantially overcome the deficiencies inherent in present vibration isolation systems by modifying the dynamic response of the actuator using local displacement feedback control, allowing stable vibration isolation to be achieved at lower frequencies without comprising high frequency isolation.

According to one aspect of the invention we provide an inertial actuator assembly comprising an actuator chassis adapted to be secured in use to a structure subject in use to external vibration forces, a proof mass (m_a) supported with respect to the chassis by a proof mass resilient means, and a force generating transducer means acting between the chassis and the proof mass for subjecting in use the proof mass to a force (f_a) applied relative to the chassis, a controller arranged to control in use the excitation of the transducer means, characterised by a feedback means $H(j\omega)$ responsive to a measurement of the displacement (x) of the proof mass relative to the chassis, the controller being arranged to modify the excitation of the force generating transducer means in response to a feedback signal from the feedback means.

Preferably the measurement of displacement is provided by an internal displacement sensor.

Preferably the internal displacement sensor is selected from the group: an electrostatic sensor; an electrical resistance sensor; a capacitive sensor; an inductive sensor; an optical sensor. In a preferred embodiment the internal displacement sensor is a strain gauge.

In order to adjust the natural frequency of the actuator the feedback signal is preferably proportional to the measurement of the displacement.

In order to overcome the problem of static sag associated with low stiffness and provide a self-levelling effect, the feedback signal can be arranged to be proportional to the integral of the measurement of the displacement.

In order to modify the damping of the actuator and control its behaviour at resonances, the feedback signal can be arranged to be proportional to the derivative of the measurement of the displacement.

Preferably, however, the feedback signal should be a combination of a signal proportional to the displacement, a signal proportional to the integral of the displacement and a signal proportional to the derivative of the displacement.

In a preferred embodiment the actuator chassis comprises a casing.

Preferably the force generating transducer means is selected from the group: an electromagnetic motor; a pneumatic motor; an electrostatic motor. In one preferred embodiment the force generating transducer means comprises an electromagnetic motor.

Preferably the inertial actuator comprises a temperature sensor, which, for example, may be configured to prevent overdriving the actuator or to

compensate for variations in the response of the system due to temperature fluctuations.

Preferably the inertial actuator also comprises a stop mechanism adapted to restrict the motion of the proof mass relative to the chassis in the event of actuation control failure.

In a preferred embodiment the inertial actuator is employed to improve the stability properties of another, outer, control system by adjusting the dynamic response of the actuator.

Some embodiments of the invention will now be described, by way of example only, with reference to the accompanying drawings. In the following description 'solid' denotes a line marked 'x' and 'faint' denotes a line marked 'y':

Figure 1 Schematic of an inertial actuator and implementation of the local displacement feedback control,

Figure 2 Schematic of the cross-section of an ULTRA Active Tuned Vibration Attenuator, Taken from Hinchliffe et al [6]

Figure 3 Frequency response of the relative displacement of the proof-mass per unit actuator force of the ULTRA inertial actuator. The solid line shows the measured data, while the dashed line shows the theoretical prediction,

Figure 4(a) Predicted Nyquist plot of the open loop transfer function, inertial actuator displacement per unit secondary force, when the controller is a realistic (solid) or ideal (faint) self-levelling device based on integral displacement feedback. λ was set to 0.4.

Figure 4(b) Corresponding measured data,

Figure 5 Predicted inertial response of the system when different ideal local self-levelling feedback loop gains g_I are used: $g_I = 0$ (solid, corresponding to $\lambda = 0$, ie no control, $g_I = 60{,}000$ (faint, $\lambda = 0.4$), and $g_I = 105{,}000$ (dashed, $\lambda = 0.7$),

Figure 6 Measured relative displacement of the proof–mass per unit command force for the passive systm (control off, solid) and for two values of the integral feedback gain: $\lambda = 0.4$ (faint), and $\lambda = 0.7$ (dashed). The theoretical prediction for this response is the same as that shown in Figure 5,

Figure 7(a) Predicted Nyquist plot of the open loop transfer function, inertial actuator relative displacement per unit secondary force, when the controller is a proportional device based on a negative position feedback gain. For $\omega = 0$ the system guarantees a 6dB stability margin when $g_P = -1000$,

Figure 7(b) Corresponding measured data,

Figure 8(a) Predicted relative displacement of the inertial actuator's proof–mass per unit command force for the passive system (control off, solid) and for three values of the proportional feedback gain: $g_P = 3100$(faint), $g_P = -900$ (dashed), and $g_P = -1400$ (dotted),

Figure 8(b) Corresponding measured data,

Figure 9(a) Predicted Nyquist plot of the open loop transfer function, inertial acutuator displacement per unit secondary force,

when the controller is the derivative of the relative displacement ($g_V = 18$),

Figure 9(b) Corresponding measured data,

Figure 10(a) Predicted relative displacement of the proof-mass per unit command force for the passive system (control off, solid) and for one values of the deriative feedback gain: $g_V = 18$ (faint),

Figure 10(b) Corresponding measured data,

Figure 11(a) Predicted Nyquist plot of the open loop transfer function, inertial actuator relative displacement per unit secondary force, when the controller is a PID with proportionality gain g_P =-1000, self-levelling coefficient λ= 0.4, and derivative gain $g_V = 18$,

Figure 11(b) Corresponding measured data,

Figure 12(a) Predicted relative displacement of the proof-mass per unit command force for the passive system (control off, solid) and with the inner PID feedback controller on (faint), with g_P = -1000, λ = 0.4, and g_V = 18,

Figure 12(b) Corresponding measured data,

Figure 13(a) Predicted blocked response of the inertial actuator (solid) and the modified inertial actuator when g_P = -1000, λ= 0.4 and g_V= 18 (faint),

Figure 13(b) Corresponding measured data,

Figure 14(a) Predicted mechanical impedance of the inertial actuator (solid) and the modified inertial actuator when g_P = -1000, λ = 0.4 and g_V = 18 (faint),

Figure 14(b) Corresponding measured data,

Figure 15 Schematic of a vibration isolation system with an inertial actuator and implementation of the local control based on displacement feedback and the outer velocity feedback control,

Figure 16 Image of the core of the experimental set-up, which consists of the piece of equipment, which is mounted on top of passive rubber rings. The ULTRA inertial acutuator is directly connected to the equipment,

Figure 17(a) Predicted Nyquist plot of the loop transfer function, equipment velocity per unit command signal, when g_P = -1000, the self-levelling coefficient λ = 0.4, the derivative gain g_V= 18, and the outer velocity control feedback gain Z_D.= 60. The modified inertial actuator is directly installed on the equipment,

Figure 17(b) Corresponding measured data,

Figure 18(a) Predicted frequency response of the equipment velocity per primary excitation when no modified inertial actuator is installed (solid), when the modified inertial actuator is installed but no outer velocity feedback loop is implemented (faint), and when both the modified inertial actuator and the outer velocity feedback loop are implemented with Z_D = 60 (dashed). Under ideal conditions stability is guaranteed when $Z_D < 120$.

Figure 18(b) Corresponding measured data. In this case stability is guaranteed when $Z_D < 90$, and

Figure 19 Mechanical Impedence of the inertial actuator with inner and outer feedback loops when the local displacement feedback control and the outer velocity feedback control are implemented. In particular, g_P= -1000, λ = 0.4, g_V = 18 and Z_D = 60.

INERTIAL ACTUATOR RESPONSE

An inertial actuator has a mass, a "proof-mass", supported on a spring and driven by an external force. The force in small actuators is normally generated by an electromagnetic circuit. The suspended mass can either be the magnets with supporting structure or in some cases the coil structure. The transduction mechanism which would supply the force to the system is not modelled in detail because its internal dynamics are typically well beyond the bandwidth of the structural response.

A mechanical model of an inertial actuator is shown in Figure 1, where the effect of $H(j\omega)$ should be neglected at this stage. A proof-mass, m_a, is suspended on a spring, k_a, and a damper, c_a, and in parallel with them, the actuator force f_a drives the mass, which is also affected by the inertial force f_i (due to gravity for example). v_a and v_e are, respectively, the moving mass velocity and the base velocity. The equation describing the dynamics of the system in Figure 1 is given by

$$j\omega m_a v_a + c_a(v_a - v_e) + k_a(v_a - v_e)/j\omega = f_i - f_a, \qquad (1)$$

where v_a and v_e are complex velocities and an $e^{j\omega t}$ time dependence has been assumed. In Figure 1, x is the relative displacement between the inertial actuator's proof-mass and the inertial actuator's reference base so

that $j\omega x = v_a - v_e$. Important parameters of the inertial actuator are its resonance frequency, ω_a, which is given by

$$\omega_a = \sqrt{\frac{k_a}{m_a}} \tag{2}$$

and the actuator damping ratio, ζ_a, defined as

$$\zeta_a = \frac{1}{2}\frac{c_a}{\sqrt{k_a m_a}} \tag{3}$$

The inertial actuator used for the experiments described below was a mechanically modified version of an active tuned vibration absorber (ATVA) manufactured by ULTRA Electronics, described in detail in [6] and shown in Figure 2, from which the internal springs were removed, leaving the proof-mass (m_a = 0.24 Kg) attached to the case by eight thin flexible supports. This modification in the stiffness (so that k_a = 2000 N/m) changed the actuator resonance frequency from 73.8 Hz to 14.5 Hz. The measured damping ratio was used to estimate the damping factor as c_a = 18 N/ms^{-1}. Figure 3 shows the dynamic response of the relative displacement of the proof-mass, x, per unit actuator force, f_a, of the ULTRA inertial actuator when mounted on a rigid base. Both measured data and theoretical prediction, calculated from equation (1), are plotted, where the measured data was divided by Bl/R, where Bl is the magnetic force constant of the inertial actuator and R is the inertial actuator electrical impedance, which was found to be resistive within the frequency range of interest. This operation of scaling was necessary in order to guarantee the same units of displacement per unit force for both curves. In an electro-mechanical actuator the damping is given by the

sum of the mechanical and electromagnetic damping and the latter is increased by the fact that a voltage amplifier was used to drive the actuator.

The displacement of the proof-mass was measured using strain gauges on the suspensions. A pair of strain gauges with self-compensating temperature device was installed on opposite sides of one of the internal thin flexible supports which hold the proof-mass inside the actuator. Each strain gauge is a 5mm rectangular foil type, and consists of a pattern of resistive foil which is mounted on a backing material. The strain gauges used in the actuator are connected to a Wheatstone Bridge circuit with a combination of four active gauges (full bridge). The complete Wheatstone Bridge, which was installed inside the inertial actuator, is excited with a stabilised DC supply and with additional conditioning electronics can be zeroed at the null point of measurement. As stress is applied to the bonded strain gauge, a change of resistance takes place and unbalances the Wheatstone Bridge. This results in a signal output related to the stress value, which is proportional to the proof-mass relative displacement. As the signal value is small (a few millivolts) the signal conditioning electronics provides amplification to increase the signal level to ± 1 V, a suitable level for the active vibration isolation application.

In the following sections we will discuss how self-levelling can be implemented by feeding back the integrated displacement, which overcomes the problem of excess actuator displacement due to gravitational forces on the moving mass (i.e. static sag due to low resonance frequency). The damping of the actuator can also be modified by feeding back the derivative of the relative displacement of the inertial actuator. In addition, the inertial actuator's natural frequency can be

lowered or increased by feeding back local proportional displacement feedback with either a positive or negative gain.

INERTIAL ACTUATOR WITH SELF-LEVELLING CAPABILITIES

The self-levelling system described here uses the inherent actuator force $f_a(t)$ to level its proof-mass. The sensing element which measures the position of the actuator proof-mass relative to the inertial actuator reference plane was a strain gauge, although an optical sensor was also investigated for this purpose. The sensing element is attached so that when the sensor is in its neutral position, the moving mass is at its desired operating height. The electrical signal is integrated and amplified by the controller, providing the control effort to operate the actuation device within the inertial actuator. The system then produces a force that is proportional to the integral of the signal from the sensor.

When a force of constant magnitude is applied to the proof-mass, causing a relative deflection of the mass on its spring element, the sensor supplies an electrical signal proportional to the mass relative displacement to the integral controller. In response, the controller generates an electrical signal that continues to increase in magnitude as long as the relative displacement is not zero. The signal from the controller is applied to the inertial actuator, which generates a force in a direction that decreases the mass deflection. The force follows the controller signal and continues to increase in magnitude as long as the relative deflection is not zero. At some point in time the force will exactly equal the constant force applied on the moving mass, requiring a relative displacement of zero. The output from the sensor is zero, therefore the output from the controller no longer increases but is maintained at a constant magnitude required for the actuator to generate a force exactly equal to the constant force applied to the proof-mass. The

force exactly equal to the constant force applied to the proof-mass. The isolation system remains in this equilibrium condition until the force applied to the proof-mass changes and causes a nonzero signal to be generated by the sensing element, and the process starts all over again.

The inertial actuator with local displacement feedback control is shown schematically in Figure 1. The relative displacement x is measured and fed back to the inertial actuator through a feedback controller with frequency response $H(j\omega)$, which in the first instance is equal to $g_I / j\omega$. The control command f_c can be considered, in control terms, as the reference point [7]. If we assume that the control force is given by the sum of a control command f_c and the time integral of the measured relative displacement between the inertial actuator proof-mass and its reference base, multiplied by a gain g_I

$$f_a = f_c + g_I \int x(t)dt \tag{4}$$

then a self-levelling device is implemented.

In order to examine the stability of the closed-loop system, composed of the inertial actuator and the self-levelling controller, the open loop gain was computed. It is given by the product of the plant response, $G(j\omega)$, (measured relative displacement per unit control force, x/f_a, obtained from equation (1) by imposing $f_i = 0$ and $v_e = 0$, since it is assumed to be mounted on a rigid base) multiplied by the control law $H(j\omega) = \frac{g_I}{j\omega}$

$$G(j\omega)H(j\omega) = \frac{1}{\left(-\omega^2 m_a + j\omega c_a + k_a\right)}\left(\frac{g_I}{j\omega}\right) . \tag{5}$$

The faint line in Figure 4(a) shows the calculated Nyquist plot, when g_I is equal to 60,000 in equation (5), and the corresponding experimental Nyquist plot is shown in Figure 4(b). It can be noted that the system is conditionally stable and the Routh-Hurwitz criterion can be used to show that the system is only stable if $\lambda < 1$ [8], where

$$\lambda = \frac{g_I}{2\zeta_a \omega_a k_a} \quad . \tag{6}$$

When g_I is equal to 60,000, the corresponding λ is equal to 0.4, which also coincides with the negative real part of $G(j\omega)H(j\omega)$ when the imaginary part is zero in Figure 4. The low frequency measurements in Figure 4(b) cannot be considered very reliable because of noise limitations, even though the general behaviour of the open loop system is clear, including the behaviour due to the real integrator. In a real system, the integrator's control law is not described by equation (5), but more realistically by an equation that includes a cut off frequency (at 1.5 Hz in this case), a finite DC magnitude, and a phase shift at DC of 0°, rather than 90°, as in the ideal case described by equation (5). A realistic expression for such control law is given by

$$H_1(j\omega) = \frac{g_I}{1 + j\omega 0.106} \quad . \tag{7}$$

Consequently, the ideal open-loop system response described by equation (5) is then replaced by a more realistic equation given by

$$G(j\omega)H_1(j\omega) = \frac{1}{\left(-\omega^2 m_a + j\omega c_a + k_a\right)} \frac{g_I}{(1 + j\omega 0.106)} \quad , \tag{8}$$

which shows that at DC the Nyquist plot starts at $\frac{g_I}{k_a}$ on the positive real axis, and then behaves as shown by the solid line in Figure 4(a).

The response of the actuator to an inertial force, f_i, can be computed by setting the control command to zero. The relative displacement x per unit inertial force f_i, when an ideal self-levelling device is implemented, is then given by

$$\frac{x}{f_i} = \frac{1}{-\omega^2 m_a + j\omega c_a + k_a + H_1(j\omega)}, \qquad (9)$$

whose behaviour is plotted in Figure 5 for different values of the local displacement feedback gain g_I. Without integral displacement feedback (solid line), the response of the system to a static force is equal to $1/k_a$, while with ideal integral displacement feedback it tends to zero, which shows that the servo action of the feedback controller will compensate for any static load. In realistic implementations, as described by equation (9), the static deflection is equal to $1/(k_a + g_I)$. The low frequency behaviour is important because it determines how well the system performs in cases like an aircraft manoeuvre or a vehicle turn. In other words, besides counter-balancing the sagging effect due to gravity, the system must be able to centre the proof-mass and prevent it from banging against the stop-ends during manoeuvres. For example, without control the relative displacement of the proof-mass, due to the gravitational force $f_i = m_a g$, where $g = 9.8$ ms^{-2} is the gravitational acceleration, on the spring k_a is given by $x = \frac{f_i}{k_a} = 1.2$ mm, while with the self-levelling control the relative displacement is equal to $x = \frac{f_i}{k_a + g_I} = 38$ μm. In case

of a $10g$ manoeuvre the relative displacement without control would be an unsatisfactory 11.8 mm, while with control this distance would be reduced to 0.38 mm. However, at the inertial actuator resonance frequency, enhancement of the response is experienced and this enhancement increases with the gain g_I, until the system becomes unstable. When the actuator stiffness, k_a, decreases, the critical value of the gain g_I decreases as well and therefore in order to have the same stability margin, lower gains are needed.

Figure 6 shows the experimental proof-mass relative displacement x per unit control command f_c, which is given by

$$\frac{x}{f_c} = \frac{1}{-\omega^2 m_a + j\omega c_a + k_a + H_1(j\omega)} \quad , \tag{10}$$

which has the same form as equation (9) whose theoretical relative displacement per unit force is shown in Figure 5. In both theory and experiment the increase in magnitude at the resonance can be noted, which is a sign of getting closer to instability, along with an additional phase shift at low frequency.

INERTIAL ACTUATOR WITH PID CONTROL

In the previous section we saw that with a displacement sensor integral control gave a self-levelling action. In this section we discuss the physical effect of proportional and derivative control in a more general PID controller.

If the inertial actuator resonance frequency is too high for the specific application, it can be lowered using a negative direct position feedback control loop, $H_2(j\omega) = g_P$, where g_P is negative. In order to determine

whether the closed-loop system in Figure 1 is stable with such a controller, the open loop gain was computed. It is given by the product of the plant response, $G(j\omega)$, defined above, multiplied by $H_2(j\omega)$

$$G(j\omega)H_2(j\omega) = \frac{1}{-\omega^2 m_a + j\omega c_a + k_a}(g_P) \quad . \qquad (11)$$

The maximum feedback gain g_P before instability is equal to the value of the stiffness term k_a. Figure 7 shows the corresponding theoretical and experimental Nyquist plot for a value of the gain g_P that is equal to $-k_a/2$, which guarantees a 6 dB stability margin. Lowering the resonance frequency also implies that smaller values of the gain g_I are needed for self-levelling purposes. Figure 8 shows the theoretical and measured proof-mass displacement x per unit control command f_c described in equation (10) when the local feedback controller, $H_2(j\omega)$, comprises the proportional term, g_P, only. If the position feedback gain was positive, the natural frequency would be increased with no danger of instability. When negative position feedback gains are implemented, the actuator resonance frequency can be lowered, but stability issues emerge as the total system stiffness tends to zero.

The stability analysis of the closed-loop system when an ideal derivation controller, $H_3(j\omega) = j\omega g_V$, is used within the local loop, is obtained by studying the open loop transfer function

$$G(j\omega)H_3(j\omega) = \frac{1}{-\omega^2 m_a + j\omega c_a + k_a}(j\omega g_V) \qquad (12)$$

which is composed of the product of the plant response, $G(j\omega)$, times the controller. In a real implementation, the frequency response of the derivative term has got a cut-off frequency after which the input signal is multiplied by a constant gain [9]. As long as this cut-off frequency lies above the maximum frequency of interest, then $H_3(j\omega)$ can be considered as a good approximation to this part of the feedback controller when modelling realistic systems. Figure 9 shows the predicted Nyquist plot of the open loop system, described by equation (12), and the corresponding measured data. Theory and experiment agree well, and they both lie in the positive real half plane, indicating that by increasing the controller gain g_V, damping is added to the dynamics of the inertial actuator. At frequencies higher than the plotted range of interest, the experimental curve enters the third quadrant. This mainly happens because the derivative block is in reality a high pass filter [9], so its magnitude becomes constant after a certain frequency and its phase tend to zero. This indicates that in a real implementation the stability margin of the closed-loop system is reduced and the amount of damping that can be added to the system is large, but finite. An additional limitation is that the noise that is present in the measured signal is amplified by the derivative controller. Figure 10 shows the frequency response of the uncontrolled inertial actuator and the controlled system when a local derivative feedback loop is implemented. A value of the feedback gain g_V was chosen so that is equal to the uncontrolled c_a so that the overall value is doubled. The uncontrolled case is already damped appropriately, but since the self-levelling integral feedback loop tends to increase the magnitude of the resonance, an additional damping term will be required when the whole PID controller is implemented, as discussed below. The experimental measurements and theoretical predictions again agree well, indicating that using a local derivative feedback controller it is possible

to add damping and therefore change the dynamic behaviour of an inertial actuator.

If the integral displacement term, the proportional term and the derivative of the displacement are added in parallel within the local feedback controller, the control law in Figure 1 becomes of the form

$$H(j\omega) = H_1(j\omega) + H_2(j\omega) + H_3(j\omega) \tag{13}$$

which describes a typical ideal PID controller. In order to determine whether the closed-loop system in Figure 1 is stable with such a controller, the open loop gain was computed. It is given by the product of the plant response, $G(j\omega)$, multiplied by $H(j\omega)$

$$G(j\omega)H(j\omega) = \frac{1}{-\omega^2 m_a + j\omega c_a + k_a}\left(g_P + \frac{g_I}{1 + j\omega 0.106} + j\omega g_V\right) \tag{14}$$

Figure 11 shows the corresponding theoretical and experimental Nyquist plot for a value of the gain g_P that is equal to $-k_a/2$, a value of g_I which guarantees $\lambda = 0.4$, and a value of g_V = 18. The closed loop system is conditionally stable, and the stability depends on the combined choice of the proportional gain and the self-levelling gain. The curve starts off at $\frac{g_P + g_I}{k_a}$ and then intersects the real axis in its negative portion before reaching the origin. Figure 12 shows the theoretical and measured proof-mass relative displacement x per unit control command f_c for the uncontrolled inertial actuator and for the modified inertial actuator, when the local feedback controller, $H(j\omega)$, has the same value of the gains as above. In this case the inertial actuator natural frequency

was lowered to about 10 Hz and this configuration was used in the active vibration isolation problem discussed in the next section.

In summary, if it is necessary to reduce the resonance frequency of the actuator because it is greater or equal to the first structural mode of the system that needs to be isolated, this can be done with a negative position feedback gain. If this action induces unwanted deflections because of the low stiffness of the closed-loop system, then a self-levelling mechanism can be employed, which is based on a integral displacement feedback. By doing so, however, the overall system gets closer to instability and additional damping is needed. Another reason why damping may be necessary is if an outer velocity feedback is to be implemented. It was shown by Elliott *et al.* [4] that this kind of system is conditionally stable and the vicinity to the Nyquist point depends on how well damped the inertial actuator is. For these reasons the implementation of a local rate feedback control turns out to be very effective in increasing the damping of the actuator.

From Figure 1, the equation that describes the complete modified inertial actuator once the local PID feedback control, described by equation (13), is implemented, can be calculated. It is given by

$$f_t = \frac{-\omega^2 m_a}{-\omega^2 m_a + j\omega c_a + k_a + H(j\omega)} f_c - \frac{\left(j\omega m_a k_a - \omega^2 m_a c_a\right)\cdot\left(H(j\omega) + j\omega Z_a\right)}{\left(-\omega^2 m_a + j\omega c_a + k_a + H(j\omega)\right) j\omega Z_a} v_e \tag{15}$$

where $Z_a = c_a + \frac{k_a}{j\omega}$ is the mechanical impedance of the actuator suspension. Equation (15) can be grouped as

$$f_t = T_a' f_c - Z_a' v_e \tag{16}$$

where T_a' and Z_a' are the blocked response and mechanical impedance of the actuator, as modified by the local displacement feedback. Figure 13 shows the predicted and measured blocked response of the uncontrolled inertial actuator and the modified inertial actuator. At frequencies higher than the actuator resonance, the transmitted force f_t tends to the control command f_c. This means that the blocked response shows that the transmitted force f_t can be regulated using the control command f_c. Figure 14 shows the calculated and measured mechanical impedance of the actuator before and after control. When g_V increases, the mechanical impedance increases at high frequencies. The magnitude plot in Figure 14 shows that, starting from the solid line which tends, at high frequency, to c_a = 18 N/ms^{-1}, the damping of the device increases $c_a + g_V$ = 36 N/ms^{-1}. The phase plot in Figure 14 shows that above resonance, the mechanical impedance is damping dominated and the system shows a skyhook damping behaviour.

ACTIVE ISOLATION WITH THE MODIFIED INERTIAL ACTUATOR

In this section we consider the use of an inertial actuator with local feedback for the active isolation of a rigid equipment structure supported on a flexible base by a resilient mount. The arrangement is illustrated schematically in Figure 15, and is described fully by Benassi *et al.*[10,11]. It consists of a flexible steel base plate 700mm × 500mm × 2mm thick, clamped on the two longer sides, which supports a rigid equipment structure modelled as a point mass (m_e = 1.08 Kg) on which is mounted an inertial actuator. The equipment structure is supported by a mount, which has a stiffness, k_m = 20000 N/m, and damping, c_m = 18 N/ms^{-1}. The model assumes that

the system is divided into four elements: a vibrating plate acting as the base structure, a passive mount, the equipment, and the inertial actuator. The uncontrolled actuator has a resonance frequency of 14.5 Hz and has a damping ratio of about ζ_a = 0.4, the mounted equipment has a resonance frequency of about 21.5 Hz and a damping ratio of about ζ = 5.2%, and the vibrating base has a first resonance frequency of about 44.8 Hz and a damping ratio of about ζ = 4.8%. An inner displacement feedback loop is used to modify the response of the inertial actuator, as discussed above, and an outer velocity feedback system is used to provide active skyhook damping for the equipment, also illustrated in Figure 15.

The expression for the equipment velocity as a function of the primary force f_p and the transmitted force f_t, is given by [11]

$$v_e = \frac{Y_e Z_m Y_b}{1 + Z_m (Y_e + Y_b)} f_p + \frac{Y_e (1 + Y_b Z_m)}{1 + Z_m (Y_e + Y_b)} f_t \qquad (17)$$

where Y_e is the mobility of the equipment structure, Y_b is the mobility of the base structure and Z_m is the mechanical impedance of the mount. Since the equipment structure is assumed to behave entirely like a rigid body of mass m_e, its input mobility is equal to $Y_e = 1/(j\omega m_e)$. The mount is assumed to have a negligible mass, and so without loss of generality its impedance can be written as

$$Z_m = \frac{k_m}{j\omega} + c_m \qquad (18)$$

where k_m is the mount's stiffness and c_m its damping factor, both of which may be frequency dependent. Substituting equation (16) into (17), the

expression for the equipment velocity, when the modified inertial actuator is attached on the equipment, is given by

$$v_e = \frac{Y_e Z_m Y_b}{1 + Z_m(Y_e + Y_b + Y_e Z_a' Y_b) + Y_e Z_a'} f_p + \frac{Y_e T_a'(1 + Y_b Z_m)}{1 + Z_m(Y_e + Y_b + Y_e Z_a' Y_b) + Y_e Z_a'} f_c \tag{19}$$

If the control law of the outer feedback loop is assumed to take the form $f_c = -Z_D v_e$, where Z_D can be interpreted as the desired impedance of the outer feedback system, then equation (19) can be used to derive the equipment velocity per primary force with both feedback loops as given by

$$v_e = \frac{Y_e Z_m Y_b}{1 + Z_m(Y_e + Y_b + Y_e Z_a' Y_b) + Y_e Z_a' + Y_e T_a'(1 + Y_b Z_m) Z_D} f_p \tag{20}$$

Figure 16 shows the active isolation system used in the experimental work. It consists of an aluminium mass acting as the equipment structure, two mounts placed symmetrically underneath the aluminium mass and a modified ULTRA inertial actuator to produce the control force. The values of the gains within the PID controller were chosen in order to provide the modified inertial actuator described in Figure 12(b).

The aluminium mass had been previously shown [12] to behave as a rigid body up to 1000 Hz, which is well above the maximum frequency of interest in this experimental study. This system is attached to a flexible plate made of steel. Further details on the passive mount system are given by Gardonio *et al.* [13], and a detailed analysis of the experimental set-up is given by Benassi *et al.* [14].

The stability of the closed loop system can be assessed from Figure 17(a), which shows the predicted Nyquist plot of the open loop response of the plant, based on the modified inertial actuator on the passive isolation system and described by the second term of equation (19), and the outer velocity feedback control gain Z_D. In this configuration, a gain of $Z_D = 60$ guarantees a 6 dB stability margin. The corresponding measured data is shown in Figure 17(b), which shows that the same stability margin is guaranteed when $Z_D = 45$. Figure 18(a) shows the equipment velocity per unit primary excitation for the uncontrolled case and for different gains in the outer feedback loop. There is a difference between the equipment-dominated resonance frequency when no device is installed (solid line), and the new resonance frequency of the system when the modified inertial actuator is applied on top of the piece of equipment (faint line). This is due to the actuator acting as a tuned vibration neutraliser, as explained by den Hartog [15]. This "passive" effect of the modified inertial actuator with local feedback on the equipment dynamics can be seen from the response when the outer loop is not implemented ($Z_D = 0$), which shows a lowered and well damped first resonance frequency, dominated by the actuator's response, as well as a damped equipment resonance frequency. In this case, the damping effect seems to be more evident than the mass-loading effect. When the local feedback gain g_V is increased, substantial damping is added to the system and both the first and second resonances are well attenuated, while attenuation at higher frequencies is experienced for high values of the gain g_V.

Good vibration isolation conditions can be achieved at the mounted natural frequency of the equipment by the modified inertial actuator and the outer velocity feedback loop. The outer loop, with response Z_D, improves the behaviour of the equipment-dominated resonance, but it

also enhances the magnitude of the inertial actuator resonance, as expected, by up to 10 dB at 10 Hz in Figure 18. When $Z_D = 60$ (dashed line in Figure 18(a)), an impressive 24 dB attenuation is present at the equipment resonance frequency compared to the case where no device is installed.

In a real implementation the situation becomes a little more critical, as depicted in Figure 18(b). The dashed line in particular shows a higher peak at the actuator resonance, which is a sign of being closer to the unstable region. The dashed line, obtained for $Z_D = 60$, has a very good stability margin and a 22dB attenuation at the equipment resonance frequency, which implies that $Z_D = 60$ is a perfectly reasonable ambition in a real implementation. The system with both inner PID and outer velocity feedback loops thus has a good stability margin and it performs very well.

The mechanical impedance of the modified actuator with outer velocity feedback loop is given from equation (15) by substituting $f_c = -Z_D v_e$

$$Z = \frac{\left(j\omega m_a k_a - \omega^2 m_a c_a\right)\cdot\left[H(j\omega) + j\omega Z_a\right] - j\omega^3 m_a Z_a Z_D}{\left(k_a + j\omega c_a - \omega^2 m_a + H(j\omega)\right) j\omega Z_a} \qquad (21)$$

which is plotted in Figure 19 for the same values of the PID gains used in the experiments and an outer velocity gain of $Z_D = 60$. It can be noted that the actuator impedance $Z = f_t / v_e$, past the first resonance frequency, tends to the desired impedance plus the derivative gain and the mechanical damping factor, $Z_D + g_V + c_a = 96$ N/ms^{-1}, which indicates that the overall system, composed of the modified inertial actuator with outer feedback loop, is similar to a skyhook damper.

SUMMARY

In using an inertial actuator for active vibration isolation, resonance frequency should be lower than the first natural frequency of the system under control and it should be well damped. Actuators with very low resonance frequencies, however, have large static displacements due to gravity. To solve this problem, a new device has been disclosed. It is an inertial actuator and has a local PID feedback loop which uses the measurement of the relative displacement between the actuator chassis and the actuator moving mass. The control law is the sum of an integral term, which provides self-levelling and solves the sagging problem, a derivative term, which provides the device with sufficient initial damping to guarantee a very good stability margin, and a positive or negative proportional term, which determines the actuator resonance frequency.

It was found from the simulations and the experiments that the new device is effective in actively isolating a piece of equipment from the vibrations of a base structure. Although the overall system is conditionally stable, very good performance can be achieved. Using negative proportional feedback loop gains, it is possible to lower the resonance frequency of the inertial actuator. Finally, damping can be added through the derivative component of the PID controller. In summary, it is possible to change the dynamic response of an inertial actuator using a local PID feedback controller and when this system is applied as a vibration isolator, the results have been shown to be very good.

REFERENCES

1. C.E.CREDE 1995, *Shock and Vibration Handbook*, C.M.Harris, ed., McGraw Hill, New York. Theory of Vibration Isolation, Chapter 30.

2. E.E.UNGAR 1992, *Noise and Vibration Control Engineering*, L.Beranek and I.L.Ver, eds., Wiley, Chichester. Vibration Isolation, Chapter 11.

3. D.KARNOPP 1995, *ASME J. Mech. Des.*, **117**, 177-185. Active and Semi-active Vibration Isolation.

4. S.J.ELLIOTT, M.SERRAND and P.GARDONIO 2001, *ASME Journal of Vibration and Acoustics*, **123**, 250-261. Feedback stability limits for active isolation systems with reactive and inertial actuators.

5. R.W.HORNING and D.W.SCHUBERT 1988, *Shock and Vibration Handbook*, C.M.Harris, ed., McGraw Hill, New York. Theory of Vibration Isolation, Chapter 33.

6. R.HINCHLIFFE, I.SCOTT, M.PURVER, and I.STOTHERS 2002 *Proc. ACTIVE2002 Conference, Southampton, U.K.*, 15-17 July 2002. Tonal Active Control in Production on a Large Turbo-Prop Aircraft.

7. G.F.FRANKLIN 1994, *Feedback Control of Dynamic Systems*, Addison-Wesley, 3rd Ed.

8. S.J.ELLIOTT 2000 *ISVR Contract Report Nº 00/28.* Active Isolation Systems: A State-of-the-Art Study.

9. M.J.BRENNAN, K.A.ANANTHAGANESHAN and S.J.ELLIOTT 2002 *Proc. ACTIVE2002* and submitted to *ASME Journal of Vibration and Acoustics*. Low and high frequency instabilities in feedback control of vibrating single-degree-of-freedom systems.

10. L.BENASSI, P.GARDONIO and S.J.ELLIOTT 2002 *Proc. ACTIVE2002 Conference, Southampton, U.K.*, 15-17 July 2002. Equipment Isolation of a SDOF System with an Inertial Actuator using Feedback Control Strategies.

11. L.BENASSI, S.J.ELLIOTT and P.GARDONIO 2003 *Journal of Sound and Vibration*. Active Vibration Isolation using an Inertial Actuator with Local Force Feedback Control. *Accepted for publication.*

12. M.SERRAND 2000 *MPhil Thesis, University of Southampton*. Direct velocity feedback control of equipment velocity.

13. P.GARDONIO, S.J.ELLIOTT and R.J.PINNINGTON 1996 *ISVR Technical Memorandum Nº 801*. User Manual for the ISVR Isolation System with Two Active Mounts for the ASPEN Final Project Experiment.

14. L.BENASSI, S.J.ELLIOTT and P.GARDONIO 2002 *ISVR Technical Memorandum Nº 896*. Equipment Isolation of a SDOF System with an Inertial Actuator using Feedback Control Strategies – Part II: Experiment.

DEN HARTOG 1985, *Mechanical Vibrations*, Dover Publications, Inc., New York.

CLAIMS

1. An inertial actuator assembly comprising an actuator chassis adapted to be secured in use to a structure subject in use to external vibration forces, a proof mass (m_a) supported with respect to the chassis by a proof mass resilient means, and a force generating transducer means acting between the chassis and the proof mass for subjecting in use the proof mass to a force (f_a) applied relative to the chassis, a controller arranged to control in use the excitation of the transducer means, characterised by a feedback means $H(j\omega)$ responsive to a measurement of the displacement (x) of the proof mass relative to the chassis, the controller being arranged to modify the excitation of the force generating transducer means in response to a feedback signal from the feedback means.

2. An inertial actuator as claimed in claim 1 in which the measurement of displacement is provided by an internal displacement sensor.

3. An inertial actuator as claimed in claim 2 in which the internal displacement sensor is selected from the group: an electrostatic sensor; an electrical resistance sensor; a capacitive sensor; an inductive sensor; an optical sensor.

4. An inertial actuator as claimed in claim 3 in which the internal displacement sensor is a strain gauge.

5. An inertial actuator as claimed in any previous claim in which the feedback signal is proportional to the measurement of the displacement.

6. An inertial actuator as claimed in any of claims 1 to 4 in which the feedback signal is proportional to the integral of the measurement of the displacement.

7. An inertial actuator as claimed in any of claims 1 to 4 in which the feedback signal is proportional to the derivative of the measurement of the displacement.

8. An inertial actuator as claimed in any of claims 1 to 4 in which the feedback signal is any combination of a signal proportional to the displacement, a signal proportional to the integral of the displacement and a signal proportional to the derivative of the displacement.

9. An inertial actuator as claimed in any previous claim in which the actuator chassis comprises a casing.

10 An inertial actuator as claimed in any previous claim in which the force generating transducer means is selected from the group: an electromagnetic motor; a pneumatic motor; an electrostatic motor.

11. An inertial actuator as claimed in claim 9 in which the force generating transducer means comprises an electromagnetic motor.

12. An inertial actuator as claimed in any previous claim which comprises a temperature sensor.

13. An inertial actuator as claimed in any previous claim which comprises a stop mechanism adapted to restrict the motion of the proof mass relative to the chassis in the event of actuation control failure.

14. The use of an inertial actuator as claimed in any one of the preceding claims in which the inertial actuator is employed to improve the stability properties of another, outer, control system.

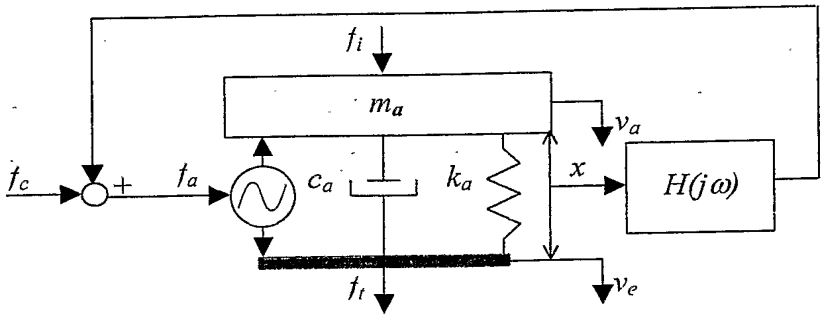

Figure 1. Schematic of an inertial actuator and implementation of the local displacement feedback control.

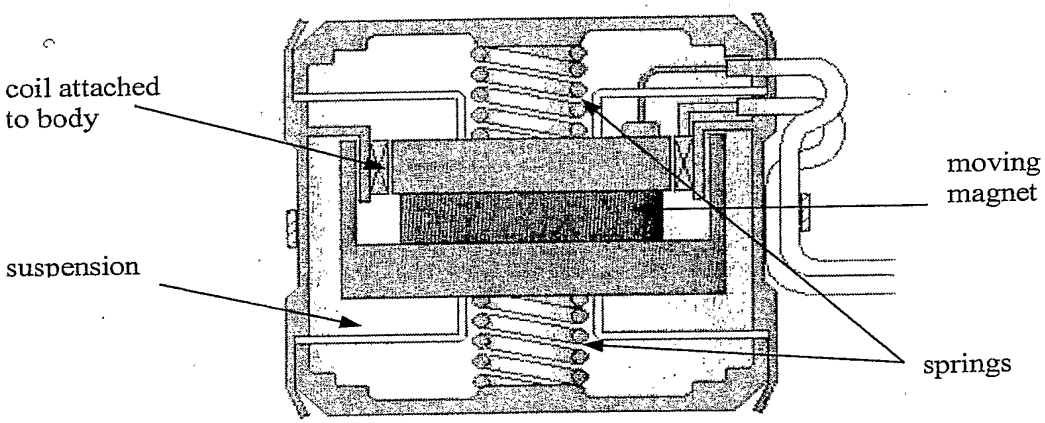

Figure 2. Schematic of the cross-section of an ULTRA Active Tuned Vibration Attenuator. Taken from Hinchliffe *et al.* [6].

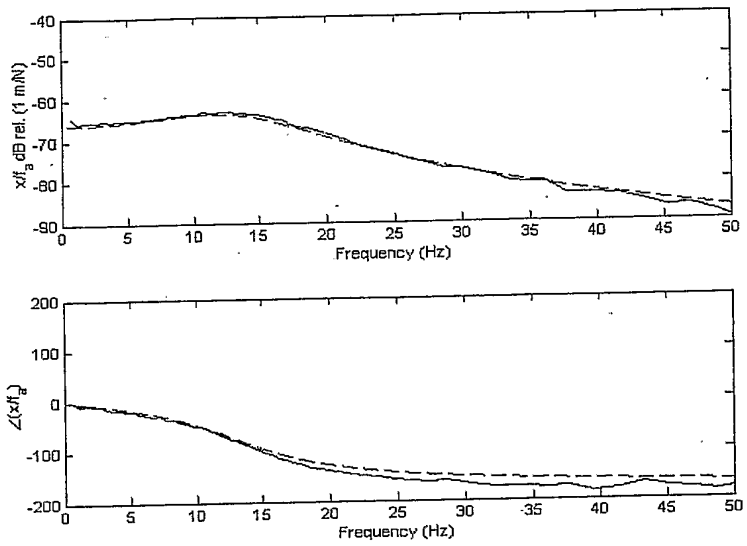

Figure 3. Frequency response of the relative displacement of the proof-mass per unit actuator force of the ULTRA inertial actuator. The solid line shows the measured data, while the dashed line shows the theoretical prediction.

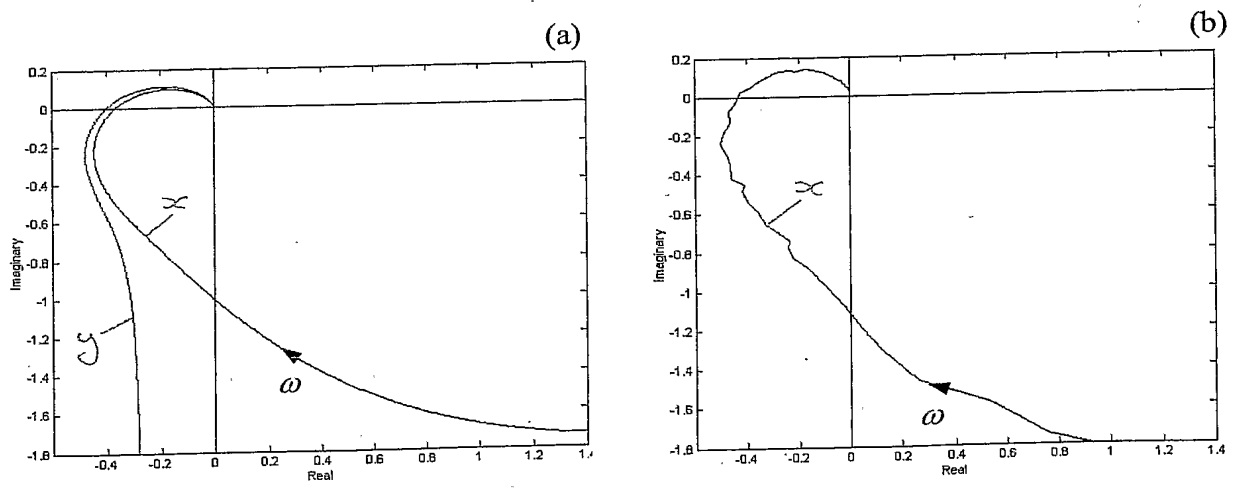

Figure 4. (a): Predicted Nyquist plot of the open loop transfer function, inertial actuator displacement per unit secondary force, when the controller is a realistic (solid) or ideal (faint) self-levelling device based on integral displacement feedback. λ was set to 0.4. (b): Corresponding measured data.

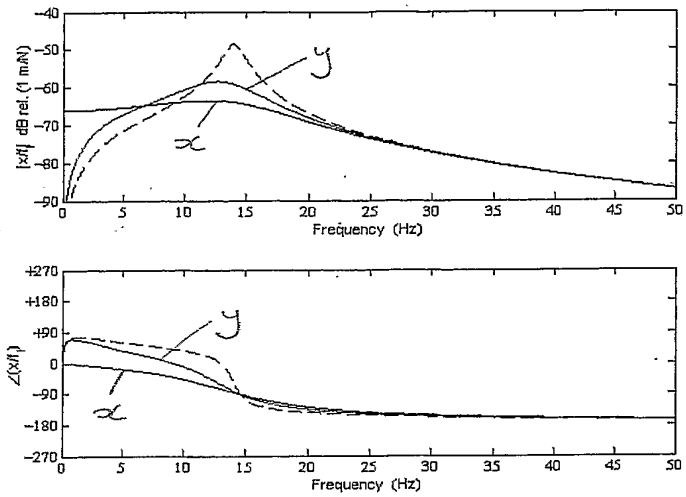

Figure 5. Predicted inertial response of the system when different ideal local self-levelling feedback loop gains g_I are used: $g_I = 0$ (solid, corresponding to $\lambda = 0$, i.e. no control), $g_I = 60{,}000$ (faint, $\lambda = 0.4$), and $g_I = 105{,}000$ (dashed, $\lambda = 0.7$).

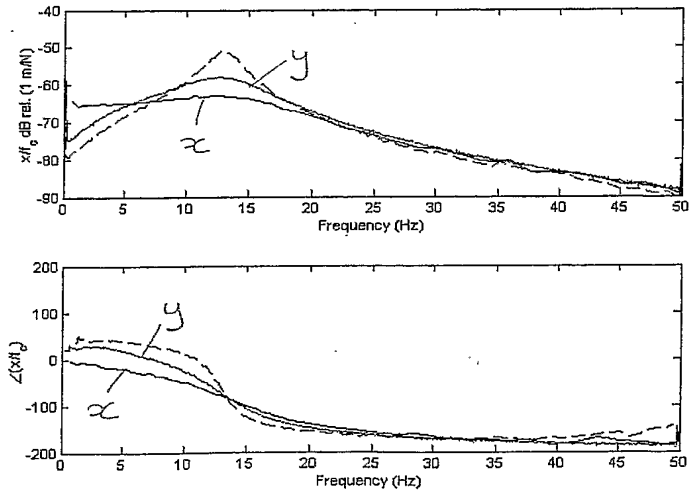

Figure 6. Measured relative displacement of the proof-mass per unit command force for the passive system (control off, solid) and for two values of the integral feedback gain: $\lambda = 0.4$ (faint), and $\lambda = 0.7$ (dashed). The theoretical prediction for this response is the same as that shown in Fig. 5.

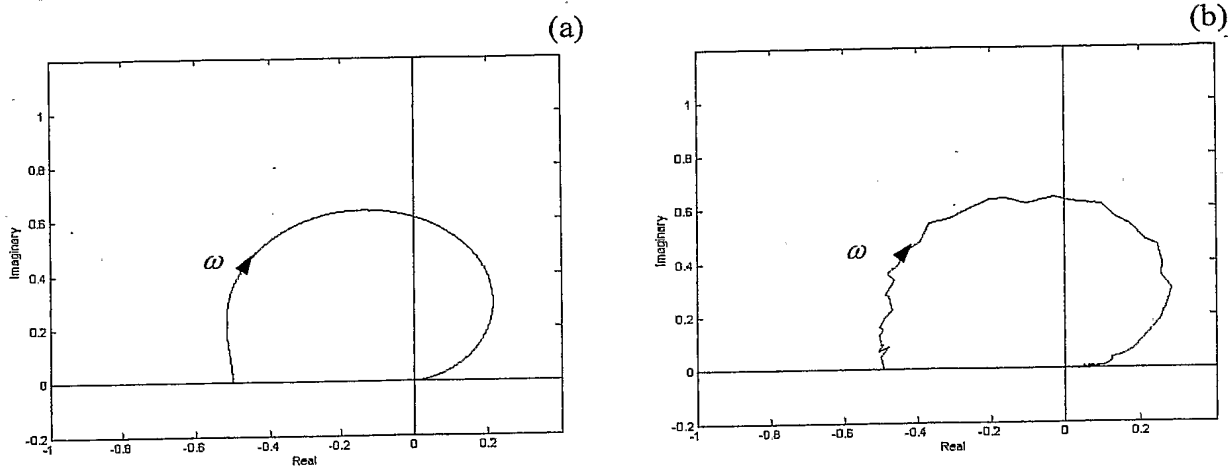

Figure 7. (a): Predicted Nyquist plot of the open loop transfer function, inertial actuator relative displacement per unit secondary force, when the controller is a proportional device based on a negative position feedback gain. For $\omega = 0$ the system guarantees a 6 dB stability margin when g_P = -1000. (b): Corresponding measured data.

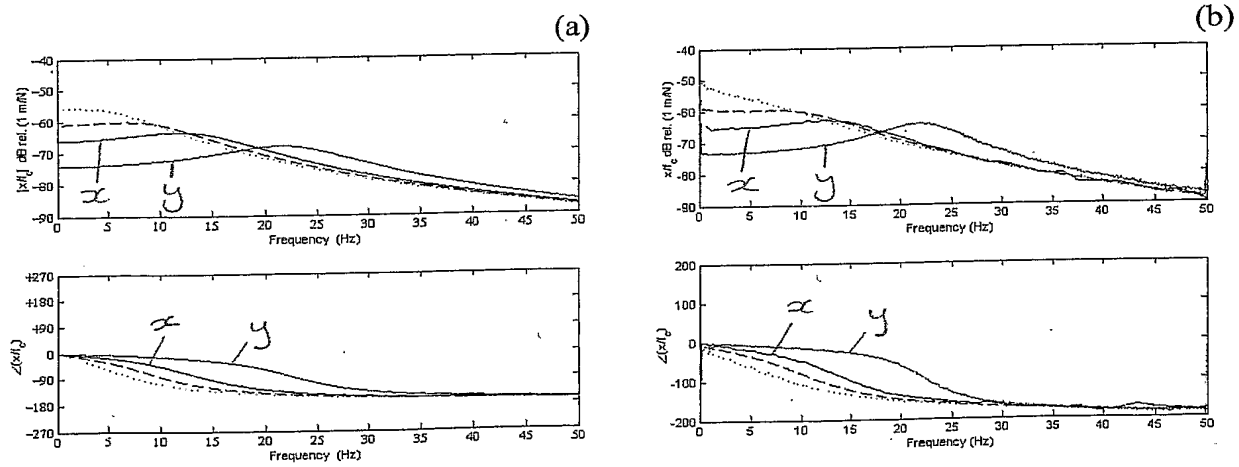

Figure 8. (a): Predicted relative displacement of the inertial actuator's proof-mass per unit command force for the passive system (control off, solid) and for three values of the proportional feedback gain: g_P = 3100 (faint), g_P = -900 (dashed), and g_P = -1400 (dotted). (b): Corresponding measured data.

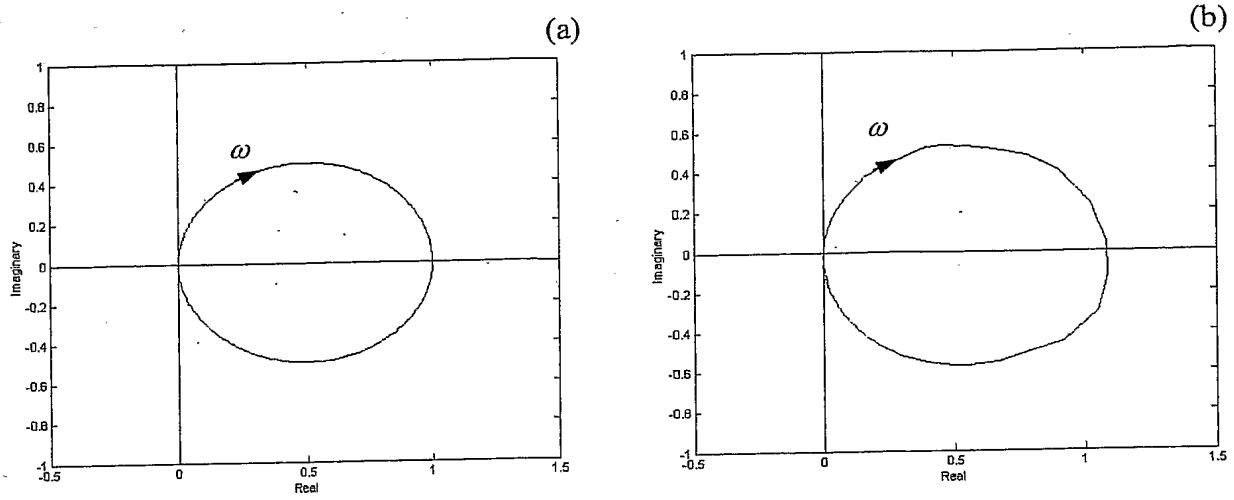

Figure 9. (a): Predicted Nyquist plot of the open loop transfer function, inertial actuator displacement per unit secondary force, when the controller is the derivative of the relative displacement ($g_V = 18$). (b): Corresponding measured data.

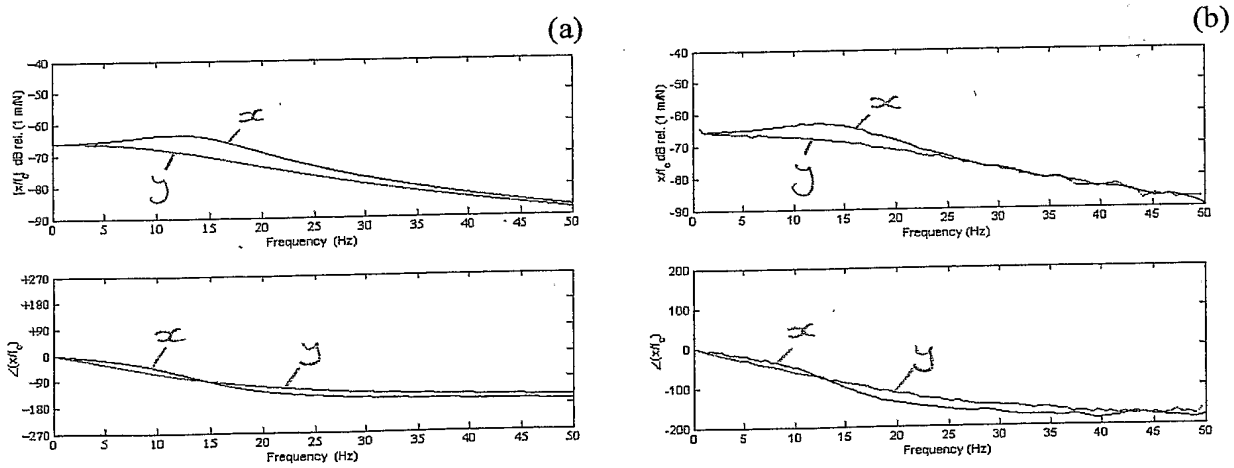

Figure 10. (a): Predicted relative displacement of the proof-mass per unit command force for the passive system (control off, solid) and for one values of the derivative feedback gain: $g_V = 18$ (faint). (b): Corresponding measured data.

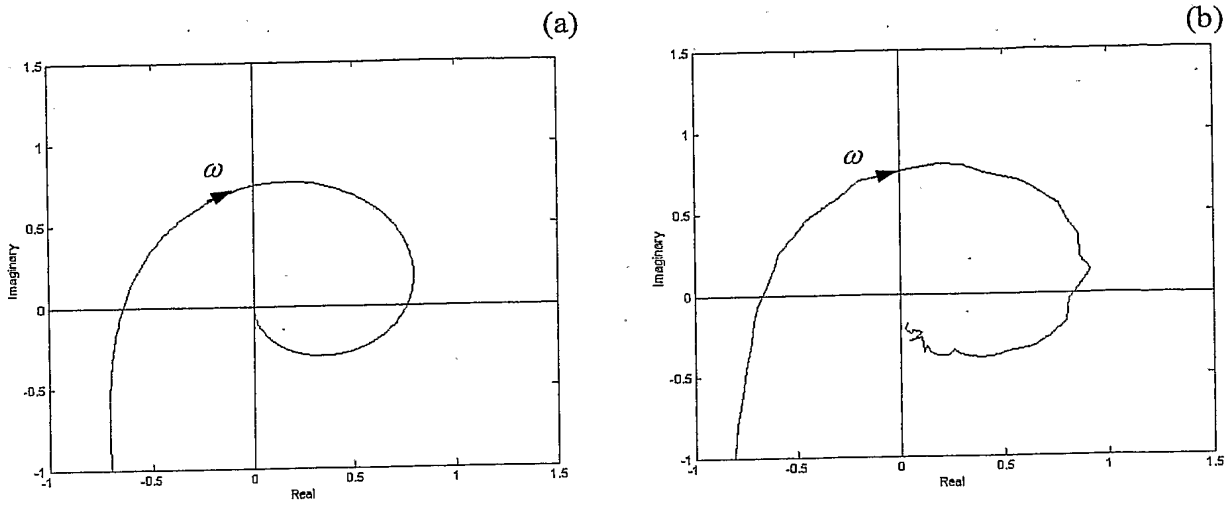

Figure 11. (a): Predicted Nyquist plot of the open loop transfer function, inertial actuator relative displacement per unit secondary force, when the controller is a PID with proportionality gain g_P = -1000, self-levelling coefficient λ = 0.4, and derivative gain g_V = 18. (b): Corresponding measured data.

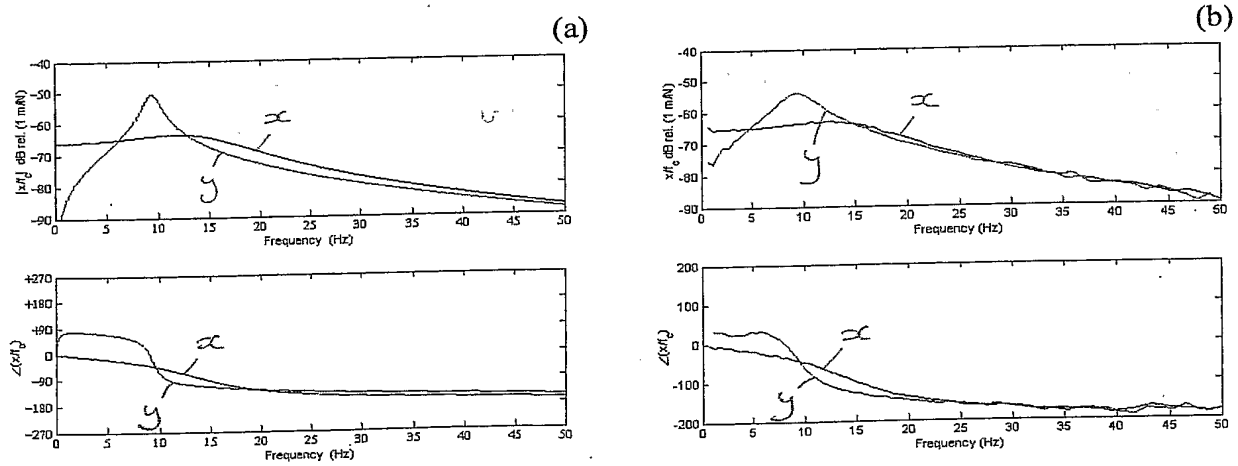

Figure 12. (a): Predicted relative displacement of the proof-mass per unit command force for the passive system (control off, solid) and with the inner PID feedback controller on (faint), with g_P = -1000, λ = 0.4, and g_V = 18. (b): Corresponding measured data.

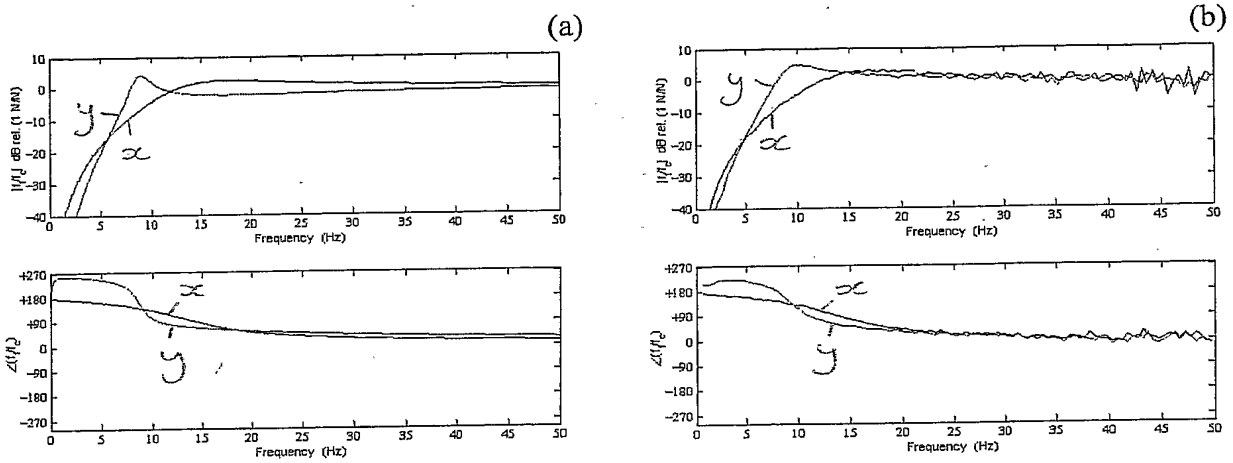

Figure 13. (a): Predicted blocked response of the inertial actuator (solid) and the modified inertial actuator when g_P = -1000, λ = 0.4 and g_V = 18 (faint). (b): Corresponding measured data.

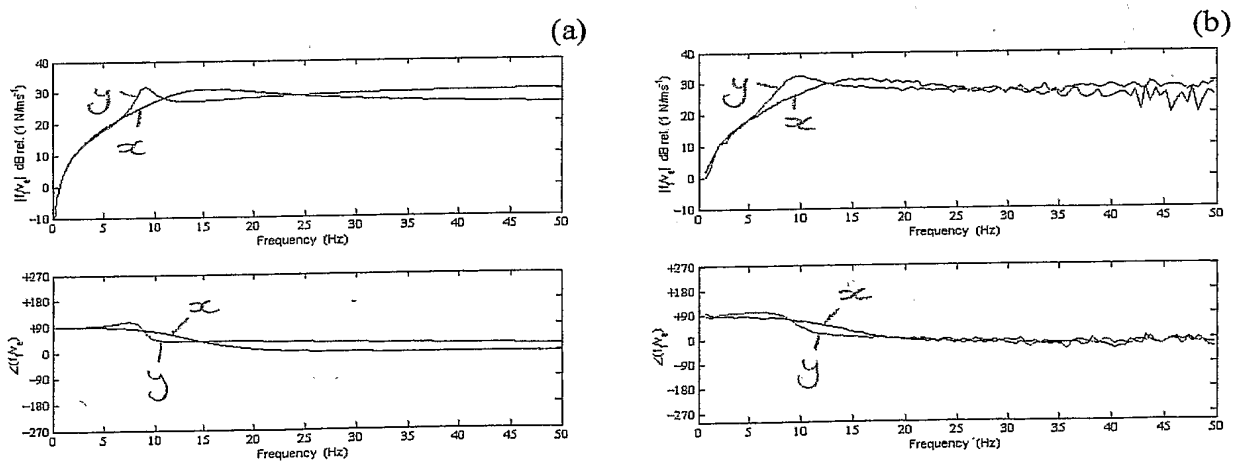

Figure 14. (a): Predicted mechanical impedance of the inertial actuator (solid) and the modified inertial actuator when g_P = -1000, λ = 0.4 and g_V = 18 (faint). (b): Corresponding measured data.

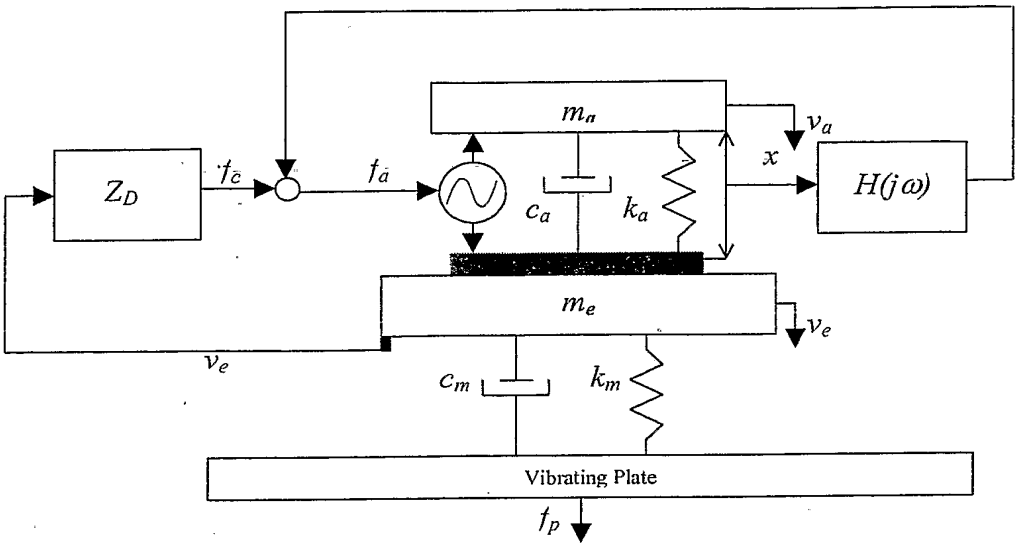

Figure 15. Schematic of a vibration isolation system with an inertial actuator and implementation of the local control based on displacement feedback and the outer velocity feedback control.

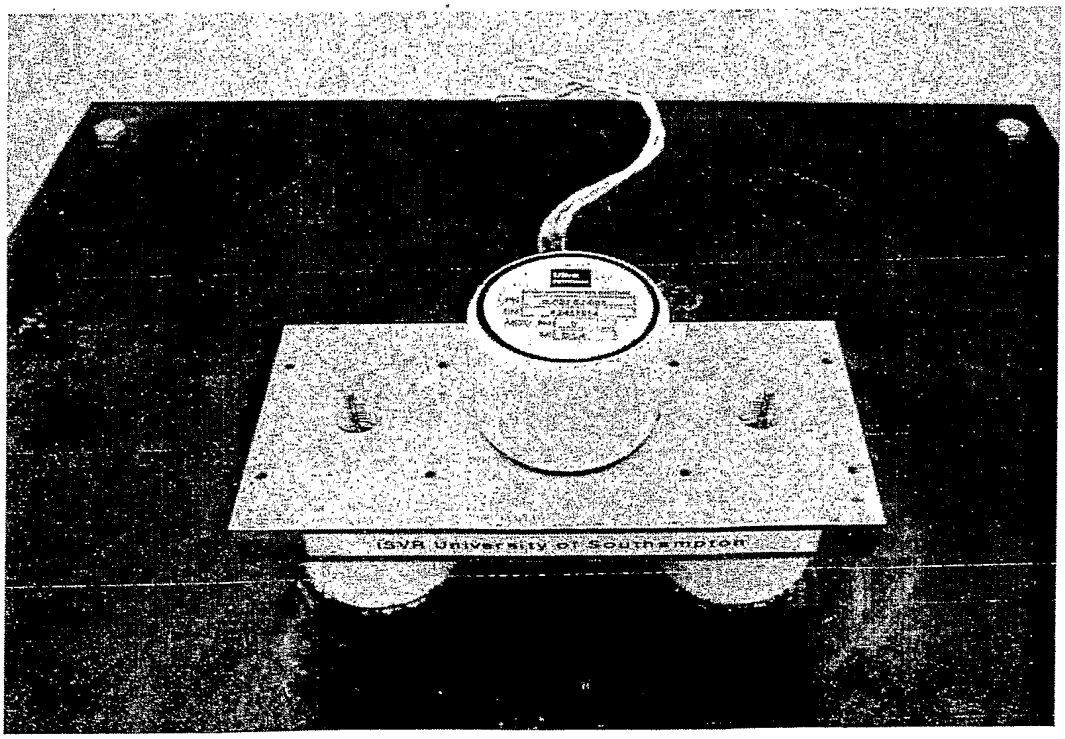

Figure 16. Image of the core of the experimental set-up, which consists of the piece of equipment, which is mounted on top of passive rubber rings. The ULTRA inertial actuator is directly connected to the equipment.

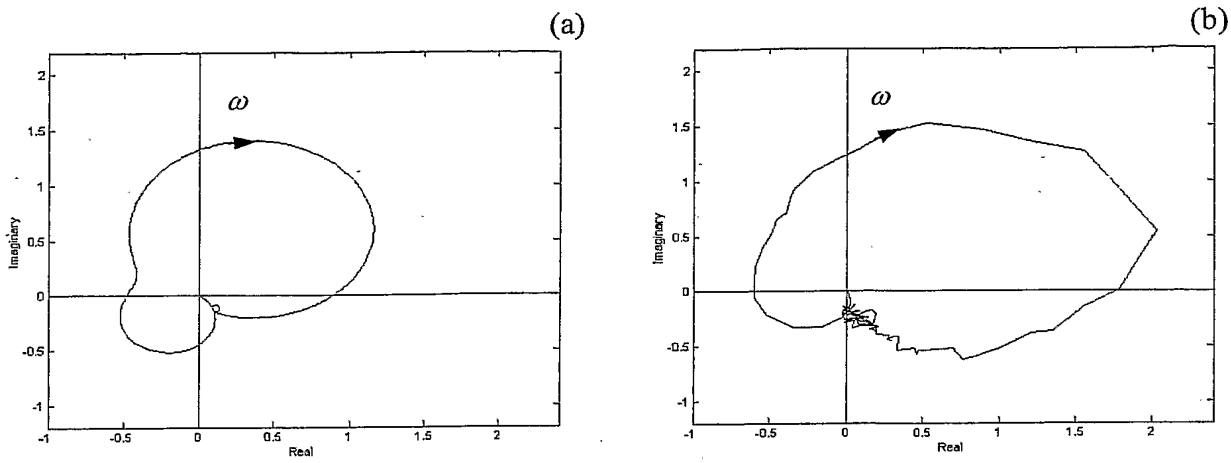

Figure 17. (a): Predicted Nyquist plot of the open loop transfer function, equipment velocity per unit command signal, when g_P = -1000, the self-levelling coefficient λ = 0.4, the derivative gain g_V = 18, and the outer velocity control feedback gain Z_D = 60. The modified inertial actuator is directly installed on the equipment. (b): Corresponding measured data.

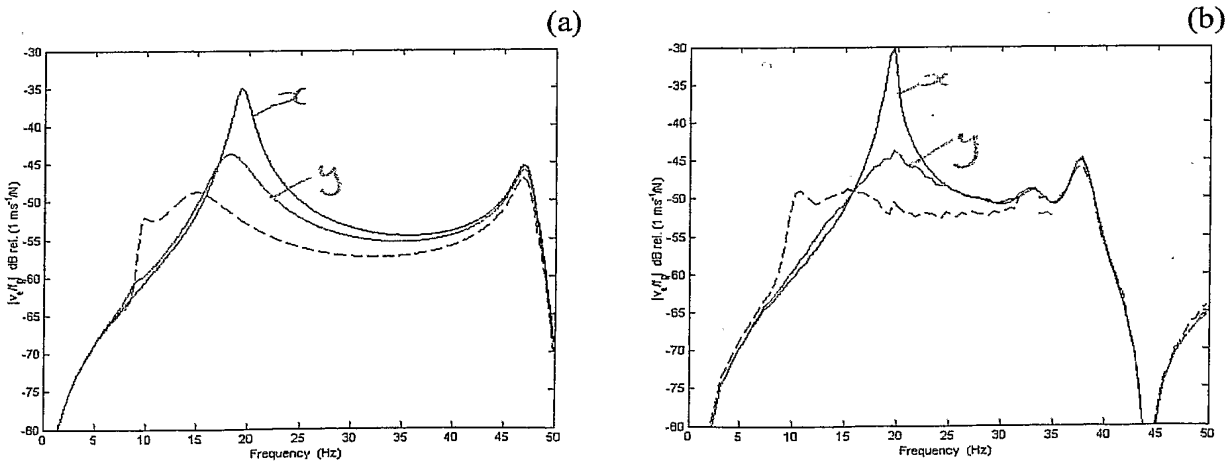

Figure 18. (a): Predicted frequency response of the equipment velocity per primary excitation when no modified inertial actuator is installed (solid), when the modified inertial actuator is installed but no outer velocity feedback loop is implemented (faint), and when both the modified inertial actuator and the outer velocity feedback loop are implemented with Z_D = 60 (dashed). Under ideal conditions stability is guaranteed when Z_D < 120. (b): Corresponding measured data. In this case stability is guaranteed when Z_D < 90.

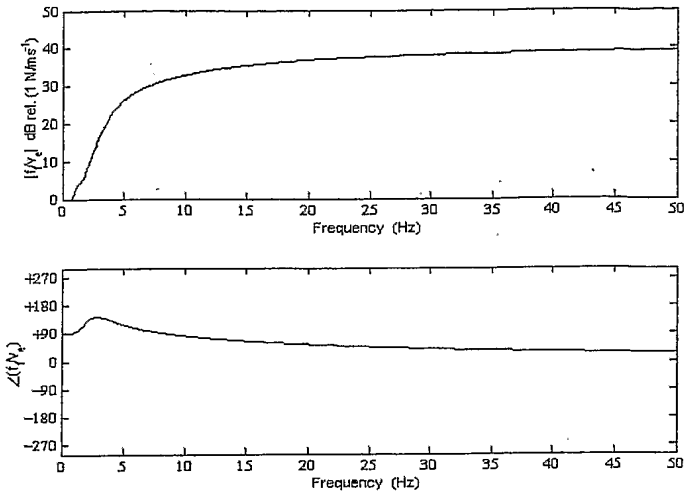

Figure 19. Mechanical Impedance of the inertial actuator with inner and outer feedback loops when the local displacement feedback control and the outer velocity feedback control are implemented. In particular, g_P = -1000, λ = 0.4, g_V = 18 and Z_D = 60.